

The prediction of chemical reactivity from first principles: Collision and reaction dynamics

Antonio Aguilar^{1,2}, Margarita Albertí^{1,2}, Jaime de Andrés^{1,2}, Xavier Giménez^{*1,2} and Josep M. Lucas^{1,2}

1. Departament de Química Física, Universitat de Barcelona

2. Centre Especial de Recerca en Química Teòrica, Parc Científic de Barcelona

Abstract

Experimental measurements and theoretical calculations on the dynamics of atomic and molecular collisions are reviewed. Experiments focused on ion-atom and ion-molecule intermediate energy collisions, for which total, state-to-state cross-sections and polarization fractions leading to spin-polarized integral cross-sections were measured from luminescent emissions on a molecular beam machine. Results were successfully interpreted in terms of non-adiabatic couplings between several electronic states of the collision partners. Theoretical calculations of chemical reactions, using quasiclassical as well as recently developed approximate and exact quantum techniques, provided both fully converged, quantum-mechanical benchmark results for several triatomic systems and a thorough analysis of dynamical features of systems ranging from triatomic to pentaatomic, for virtually all relevant quantities.

Keywords: Reaction dynamics, molecular beams, potential energy surfaces, quasiclassical trajectories, reactive quantum dynamics.

Resum

Aquest treball fa una revisió de mesures experimentals i càlculs teòrics sobre la dinàmica de col·lisions i reaccions moleculars. Els experiments se centren en col·lisions, a energies intermèdies, que involucren sistemes del tipus ió-àtom i ió-molècula, per les quals es mesuren seccions eficaces totals, estat a estat, així com aquelles que discerneixen les diferents contribucions del moment angular d'espín. Els resultats obtinguts s'interpreten satisfactòriament en termes d'acoblements no adiabàtics entre els diferents estats electrònics dels sistemes col·lisionants. Els càlculs teòrics utilitzen la metodologia quasiclàssica, així com metodologies mecanoquàntiques recentment desenvolupades, tant aproximades com exactes. S'han obtingut resultats totalment convergits per sistemes tipus, mentre que s'han analitzat, de manera detallada i extensiva, les característiques dinàmiques de sistemes triatòmic, tetraatòmic i pentaatòmic.

I. Introduction

Molecular dynamics of few-body processes, which cover elastic, inelastic and reactive collisions, is a very active sub-field of Physical Chemistry / Chemical Physics and has advanced greatly during the last three decades [1-5]. This advance originated in the perception that the rigorous prediction of chemical reactivity required study in the realm of molecular collisions (molecular scattering theory), in addition to structure (static) analyses. As a result, a wide range of non-equilibrium properties, such as rate constants, integral and differential cross-sections, transport coefficients etc., as well

as their state-to-state counterparts, have been elucidated for a great variety of collision systems in unprecedented detail and accuracy. Moreover, the strong interplay between theory and experiments, which may well be one of the highest in molecular sciences, provides a unique framework for comparison and interpretation.

The current state-of-the-art is that, experimentally, single collision measurements at the femtosecond time scale are being (almost) routinely produced, which means specific rovibrational quantum states can be singled out, whereas, theoretically, the rigorous framework provided by quantum scattering theory has both reached the full convergence regime for simple-to-moderate polyatomic chemical reactions and made available fairly accurate data for truly complex molecular systems.

The natural outcome of these studies is a much more detailed understanding of collision and reaction mechanisms,

* Author for correspondence: Xavier Giménez. Departament de Química Física. Universitat de Barcelona. Martí i Franquès, 1. 08028 Barcelona, Catalonia (Spain). Tel. 34 934021239. Fax: 34 934021231. Email: xgimenez@qf.ub.es. Website: www.qf.ub.es

of direct use in advanced studies of chemical dynamics and kinetics, i.e. the most accurate route towards a profound understanding of chemical reactivity. In addition, the availability of this information provides fine-structure data on atomic and molecular systems, which are expected to have a major influence in more applied, rapid-growth areas such as laser science, nanoscience, materials science, spectroscopic methods (including medical applications), as well as biophysics and biochemistry [4, 5].

The purpose of this paper is to review the authors' recent research on the subject. This includes experimental, molecular-beam studies of ion-atom collisions (plus very recent ion-molecule experiments), theoretical calculations on non-adiabatic processes in ion-atom intermediate energy processes, plus quasi-classical, and exact and approximate quantum mechanical studies of polyatomic chemical reactions (specifically, three-, four- and five-center chemical reactions, at varying degrees of accuracy).

The experimental work performed so far focuses on:

- the measurement of excitation and charge-transfer total cross-sections in ion-atom collisions, state-to-state resolved cross-sections and polarization fractions as a function of collision energy,
- interpreting and modeling the above collision processes using theoretical tools, and
- experimental studies of ion-molecule reactions at intermediate collision energies.

The aim of the theoretical studies is four-fold:

- To develop and implement new algebraic and numerical methodologies, so as to increase the computational performance and the applicability range of previous methods,
- To provide benchmark data for the testing of potential energy surfaces and approximate dynamical methods,
- To characterize the scattering dynamics of processes for which this information is lacking, and
- To interpret and model the new results in terms of simplified theories, gaining understanding and extrapolating general rules in order to increase predictive capacity.

The specific processes reviewed here fall into one or more of the above categories. For instance, triatomic systems such as $\text{Ne} + \text{H}_2^+$, $\text{He} + \text{H}_2^+$ and $\text{F} + \text{H}_2$ were studied to test new methodological advances, provide new data, test more approximate treatments, check the potential energy surface accuracy and model several of their dynamical features. Results for the $\text{Ar}^* + \text{CIF}$ system focus, however, on characterizing the excited electronic state reactivity and model the angular-momentum related features. Finally, work on tetraatomic systems such as $\text{BO} + \text{H}_2$, as well as the pentaatomic $\text{C}_2\text{H} + \text{H}_2$, centers mainly on providing new data and understanding the role of non-reactive bonds.

The remainder of the paper is organized as follows: Section II describes the experimental set-up for the measurements given, Section III briefly discusses the main aspects of the theoretical methodology, and Section IV shows some of the main results, both experimental and theoretical. Future prospects are briefly discussed in Section V. Finally, Section VI summarizes and concludes.

II. Experimental set-up

Our experimental machines now in use or under construction are of the crossed molecular-beam type. They are assembled from a variety of subsystems, which may be repeated or even moved among the different set-ups. For these reasons, the following description is based on the various subsystems. Later on, the different assemblies will be briefly described. Figure 1 shows a typical experimental set-up.

Chambers and high-vacuum generation / measurement

All chambers were built of welded 316L stainless steel, along with some dural elements where necessary. Flanges and collars are standard in their geometry, allowing for exchange and high versatility. Vacuum was generated by tandem rotary / oil diffusion pumps, over-dimensioned to reduce residual contamination. Oil backstreaming was prevented thanks to water-, freon- or LN_2 -cooled baffles. Cryogenic traps were also used to catch eventual residual beams, and Pirani and Penning-type vacuum gauges were used throughout. Experiments were run at background pressures of 10^{-6} torr or lower, so as to ensure sufficiently long mean free paths within each of the beams.

Effusive atom or molecule beam generators (volatile solids)

Atom or molecular beams are generated from thin-walled ovens, made of refractory stainless steel or carbon, depend-

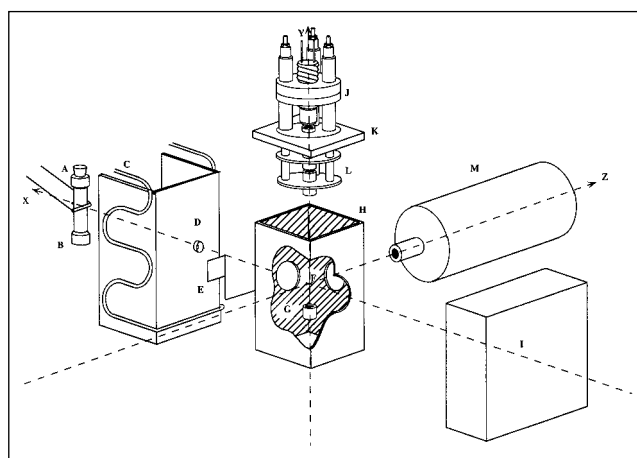


Figure 1. Diagram of the experimental apparatus. A: metal oven, B: thermocouple, C: water tubes, D: metal-catching baffle, E: shutter, F: scattering center, G: Faraday cup, H: scattering center optical center, I: liquid nitrogen trap, J: ion beam generator mounting, K: ion generator, L: Einzel electrostatic lens system, M: optical system. X, Y, and Z: vacuum chamber axes.

ing on the working temperature range [6]. The ovens are clamped to a pair of water-cooled conductors fed with high-intensity AC current *via* a triac and a step-up transformer. A 0.5 or 1mm hole in the oven wall allows the inner vapor to efflux in a beam which is collimated afterwards.

Beams composed of neutral species may be generated by simple evaporation of the metal or salt (e.g. Na, ZnCl₂), or by heating a reactive mixture that produces the desired species through displacement or dissociation processes such as:



In the near future, an electrical discharge device will be assembled, to let decompositions of the type SnCl₂ → SnCl + Cl take place in the beam. The beam is directly characterized in experiments involving alkaline metals, simply by installing a surface ionization detector somewhere in the beam path.

Gas-beam generators

Gas beams (either pure or target / carrier gas mixtures) are generated by supersonic efflux through an adequate nozzle, and further collimated by passing through a skimmer. Experiments performed with excited species require an additional electron beam (prepared from an electron generator), which is crossed with the target. Application of an electrical field enables the ions thus formed to be characterized.

Alkali ion-beam generation

Alkali-ion production is based on the thermo-ionic effect, caused by heating spodumene (an alkali-bearing aluminosilicate) pellets fixed to a tungsten foam support. They are heated by a battery-fed DC circuit *via* variac controllers. A positive potential of up to 5 keV is applied to both the support and the support bearer, thus ensuring ion extraction and expulsion.

A three-element einzel electrostatic lens system is then used to collimate the resulting beam. When necessary, the beam may be further shaped from a collimating screen mounted just before the beam-crossing volume. The scattered beam is then collected by a Faraday cup, which measures its overall intensity.

The possibility of wide changes in the operating conditions of the whole crossed-beam device required an accurate characterization of beam geometry, in particular as a function of the different extraction potentials. Thanks to this characterization, results for each condition are fully comparable.

Fluorescence measurement

Fluorescent emissions are collected either by a telescope or an optic fiber beam, directed towards a monochromator, and then to a Peltier-cooled multiplier phototube. Enhanced sensitivity, at a given wavelength, may be obtained by the

use of interference filters, instead of a monochromator. Recently, a computer-controlled data collecting card has been introduced to simplify data processing. A polarizing filter in the optic path measures eventual polarization effects.

Mass-analysis measurements

To find information on the specific mass of each collision fragment, ions formed in the collision processes are directed to a quadrupolar mass analyzer.

III. Theoretical methods

Molecular collisions at chemical energies are guided by the interaction between valence electrons, by the energy stored in the nuclear degrees of freedom (dof) and by the ability of the molecular system to transfer energy between the whole set (electronic + nuclear) of dofs. Whereas the electronic problem is treated by the methods of quantum chemistry, usually leading to the potential energy surface (PES) governing the nuclear motion, molecular dynamics accounts for events related to the nuclear degrees of freedom. Here we focus on the latter except in paragraph C), in which electronically non-adiabatic collisions are examined.

A) Classical methods

Any *ab initio* theoretical treatment of molecular collisions starts from the equations of motion associated with each specific system and works out a strategy for their solution. In principle, for full accuracy, the molecular motion in quantum mechanics should be discussed within the framework of scattering theory. However, it is easily verified that typical molecular masses lie between the applicability range of quantum and classical mechanics (i.e. the associated de Broglie wavelength takes intermediate values). In consequence, it seems more sensible to try to solve the classical equations of motion for the nuclei.

This is the origin of what are known as quasi-classical trajectory methods. These solve the Hamilton equations and assume that collisions can only start in states compatible with true quantum initial (reactant) states, whereas final (product) states are box-quantized to the relevant true quantum states. Comparison with experimental quantities often requires averaging over those dofs/quantities which are not selected by the experiments. This is usually achieved by means of Monte-Carlo sampling techniques [2,3], which require the running of a high number of classical trajectories (this being the bottleneck of classical studies). Overall, the application of this methodology is rather straightforward and robust, which may well be the main reason for its widespread use. Results appear to be semi-quantitatively correct, mainly for averaged quantities and for a large class of elementary reactions, with the added advantages of a relatively low computational cost and ease of interpretation. The quasi-classical trajectory method was used, in the present research, to tackle dynamical features of excited-state triatomic reactions, as well as combustion-related tetraatomic processes.

The obvious limitation of classical methods is that quantum mechanical features are missing. These features usually appear in the form of a correction over a background, classical reactivity. They arise from the interference phenomena caused by the wavelike nature of molecular systems, so that this correction might lead to either enhancing or inhibiting a given classical value for a dynamical quantity. One may argue that the averaged nature of most relevant dynamical quantities leads to the quenching of quantum interference, so that the resulting quantum effects become, in practice, undetectable. However, whereas these quantum effects are dominant at low, threshold energies, recent experience reveals that, for low to moderately high energies, they may be much stronger than previously expected and so show up even at the averaged quantity level [7]. In particular, relevant quantum effects are expected for systems having light masses, processes leading to long-lived complex formation, and molecular fragments characterized by large vibrational frequencies. These features will be illustrated in more detail below.

B) Quantum methods

Contrary to what happens with classical methods, purely quantum mechanical techniques are more difficult to apply computationally, and one often faces some trouble with physical interpretation. In addition, quantum algebra is not straightforward, which has led to several methodologies, based on substantially different starting strategies, being put forward over the years. These strategies have competed for the best performance [4]. Despite this, the possibility of reaching full convergence has spawned the application of quantum methods to several kinds of molecular systems.

A typical classification divides the existing methods according to whether they are based on solving the time-dependent or the time-independent Schrödinger equation. The information provided by the two methods is identical, but the numerical performances may differ substantially, since the structure of the defining differential equations is also different. In addition, the computational overload depends strongly on specific details of the methods, i.e. coordinate systems, basis functions, adiabatic or diabatic type expansions, use of variational methods, propagation techniques (both in time and position) [3] etc.. Because of this, it is difficult to establish which is the best technique for a given application, since an eventual reformulation of a given technique may lead to variations in performance.

The authors' recent work focused on several variants of time-independent techniques, since these cope better with large sets of state-to-state quantities. These methods are generally grouped into two classes, depending on the coordinate system used to write the Hamiltonian. A further division, within each class, may then be made according to specific techniques used to solve different parts of the scattering equations, as follows:

- a) Methods using Jacobi coordinates
 1. Variational solution of the scattering equations
 2. Propagation solution of the scattering equations

- a) Methods using Hyperspherical coordinates
 1. Finite basis representation (FBR) for the internal problem
 2. Hyperquantization algorithm (HA) for the internal problem

Further details about the methods used so far are also relevant. Methods based on Jacobi coordinates are formulated under reduction dimensionality schemes (in particular, freezing some angular motions). They also have in common the use of Negative Imaginary Potentials (NIP), since they have the property of absorbing the probability flux of the wavefunction reaching the configuration space region where they are placed [8]. Thanks to this property, the size of the configuration space to be explored, and so the computational expense, can be reduced. These methods have been used to perform approximate studies for up-to-pentaatomic systems.

Methods a1 and a2 differ in the solution strategy for the scattering equations. Whereas the first method uses a Kohn-type variational principle [3] to generate a linear, first-order set of equations for the expanding coefficients, the second solves a second-order radial set of differential equations using what are known as propagation, invariant embedding methods [4]. The main difference between the two strategies is the size and management of the matrices handled in the solution algorithm. Whereas the variational approach has to invert just one very large matrix (whose dimension goes easily to several thousand rows) using primary memory, the propagation method operates on several, smaller matrices (typically a few hundred rows), but makes greater use of secondary memory.

Methods based on Hyperspherical coordinates (by which the relevant coordinates are a hyperradius and $3N-4$ hyperangles, three of them describing the space orientation of the whole system; N is the number of atoms in the molecular system) have been mainly used to perform fully converged calculations on benchmark triatomic systems. The hyperspherical approach exploits the fact that, when the collision partners are close together, their interaction displays a symmetry that makes the hyperradius a quasi-separable coordinate. This makes an adiabatic-type expansion between the hyperradial and hyperangular parts of the overall motion efficient. At this point, methods b1 and b2 then differ in the solution strategy for the internal hyperangular motion.

The FBR approach is based on expanding the hyperangular motion, which is bounded-type, on the basis of delocalized sine and cosine functions. The advantage is that integrals appearing in the scattering equations are analytic and display several symmetries, which reduce their number so that they only increase linearly (instead of quadratically) with the number of base functions. However, the delocalized nature of the base functions becomes less efficient for configurations where the collision partners are well separated. This point can be alleviated with a proper base contraction. For instance, it is found that the basis arising from the diagonalization of the $[\cos^2\theta]^{-1}$ operator (θ being one of the hyper-

angular variables) gives a compact representation at large ρ (the hyperradius), provided one keeps in the expansion the base functions corresponding to the lower eigenvalues. Another way of compacting the base expansion at large ρ is to switch from two variants of hyperspherical coordinates, e.g. from Smith-Whitten (democratic, independent of the arrangement channel, those used in the present formulation of the hyperspherical approach) to Delves (arrangement-channel dependent, leading to a more compact representation at large ρ) [9]. However, it is a rather cumbersome process which is little used in actual applications.

The HA algorithm is based on an expansion of the internal motion in terms of very localized basis functions, which diagonalize the position operator when it is initially represented in terms of Jacobi polynomials. The advantage is that the resulting new base is analytically known, the discrete Hahn polynomials having the important property of preserving orthonormality, independently of the base dimension [10]. An additional simplifying feature is that the kinetic energy matrix is tridiagonal and displays several symmetric properties. Further use of truncation-diagonalization techniques renders the method very competitive.

C) Hemiquantum methods for non-adiabatic ion-atom collision processes

Theoretical calculations, to interpret our group's experimental measurements, have also been undertaken. Any prospective methodology has to take into account the possibility of including several electronic states and their corresponding coupling terms in the defining differential equations, so as to allow for electronic non-adiabatic transitions (and thus go beyond the Born-Oppenheimer approximation). An added difficulty is the relatively high collision energy at which measurements were taken.

A family of methods which take an optimal compromise between computational cost and accuracy is that termed as hemiquantum. These are mixed quantum-classical methods, in which some degrees of freedom are treated quantum-mechanically (the electronic dofs), whereas the remainder are treated classically (the nuclear dofs). Thus, the electronic motion is obtained from its total wavefunction, which is expanded as a function of a set of adiabatic molecular electronic wavefunctions, with the expanding coefficients being time-dependent and complex. The nuclear degrees of freedom are treated classically, with the interaction potential being given by the Ehrenfest theorem from the electronic wavefunction. This interaction is assumed to depend on both R , the internuclear atom-ion distance, and Θ , the polar angle, so as to account properly for both the radial and angular coupling terms of the electronic problem. This leads to a four-dimensional (nuclear position and momentum) classical problem, coupled to the N -state (electronic) quantum problem.

The collision process is studied by solving the time-dependent set of coupled differential equations, once the required initial conditions are determined: a high R value at the start (so that interatomic interactions are negligible), an ini-

tial electronic entrance channel (i.e. setting to one its corresponding coefficient in the adiabatic expansion), a value for the nuclear angular momentum (l), and a value for collision energy. The hemiquantum set of equations are time-evolved for a sufficiently long time. At this point, total inelastic excitation and electron transfer cross-sections are determined from a well-known sum of the squared modulus of the relevant expanding coefficients, for all contributing values of the orbital angular momentum, at each collision energy.

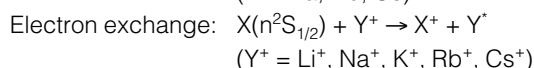
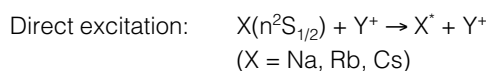
IV. Results

A. Ion-atom (molecule) collision experiments and non-adiabatic hemiquantum calculations

Most of the experiments performed by the authors focus on intermediate energy alkali ion – alkali atom collisions. These processes, widely studied since the pioneering work of Marino [11] and Aquilanti et al. [12], lead to the formation of excited atoms (either by direct excitation or by electron transfer), which in turn decay in the form of fluorescent emissions covering a wide wavelength range. Consequently, they are not only potential laser sources, but also possible dopant agents in metal-vapor lamps (so as to modify their emission spectra). Finally, these collisions may stand as good low-cost benchmarks for the testing of new theoretical methods. Work by the authors then explored previously unstudied ion-atom combinations and general scattering dynamics trends within the whole family.

The specific experimental set-up consists of a single chamber, containing the neutral atom source, an alkaline ion generator and a light-collection and analysis unit (see Fig. 1). In addition, the metal source was surrounded by a water-cooled sleeve, whereas the scattered beam was targeted towards the LN_2 trap, so as to reduce chamber contamination by alkaline metals. This let the background pressure be reduced to 10^{-7} torr.

Sodium beams were generated by simple heating, whereas Rb and Cs beams were obtained from the corresponding displacement reactions. These beams were subsequently crossed with Li^+ , Na^+ , K^+ , Rb^+ and Cs^+ ion beams, at collision energies ranging from 0.1 to 5.0 keV. Decay fluorescence signals, caused by the following processes, were detected:



Results were classified according to the degree of averaging of the quantity actually measured:

a) Total collision cross-sections

Total collision cross-sections were measured for virtually every combination of neutrals and ions. Some general points about the set of results are in order: i) the promotion of the

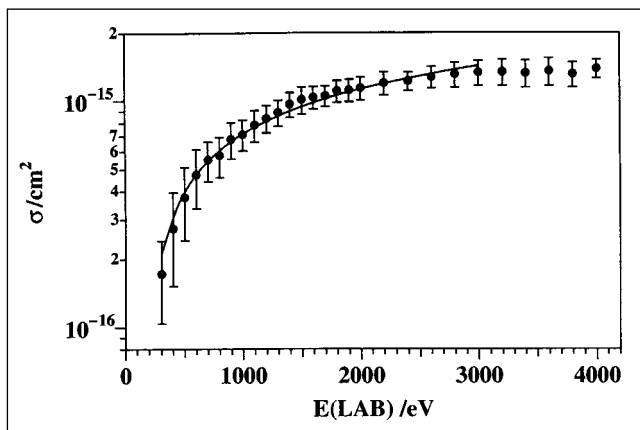


Figure 2. Total emission cross-section vs collision energy for the formation of Rb($5^2P_{3/2,1/2}$) in the Rb($5^2S_{1/2}$) + K^+ collisions. Dots represent experimental results; solid line corresponds to their fitting using the rotationally coupled Landau-Zener-Stueckelberg treatment (see refs. 13–15).

Table 1. Direct excitation and total (direct excitation + electron transfer) cross sections in collisions of alkali ion – alkali atom, at a collision energy in the laboratory frame of 2000 eV. Direct excitation of the target corresponds to the $n^2P_{1/2,3/2}$. «No» means that no signal was detected, whereas a dash indicates that the corresponding measurement has not yet been calculated.

	Li+	Na+	K+	Rb+	Cs+
Na Direct	$1.0 \cdot 10^{-17}$	–	$4.0 \cdot 10^{-16}$	$2.0 \cdot 10^{-16}$	$1.7 \cdot 10^{-15}$
Total	–	–	–	$1.0 \cdot 10^{-16}$	–
Rb Direct	No	–	$1.1 \cdot 10^{-15}$	–	$2.0 \cdot 10^{-15}$
Total	$1.05 \cdot 10^{-15}$	$1.1 \cdot 10^{-14}$	–	$3.0 \cdot 10^{-15}$	–
Cs Direct	No	–	–	–	–
Total	–	–	–	$3.5 \cdot 10^{-14}$	–

unpaired electron in the target atom to the first excited level, i.e. $X(n^2S_{1/2}) + Y^+ \rightarrow X(n^2P_{1/2,3/2}) + Y^+$ (a typical result is shown in Figure 2), is enhanced by an increase in the ion mass, whereas it is inhibited by an increase in the target mass (see Table 1); ii) the most probable transition in electron-transfer processes is the promotion to the first excited state, i.e. $X(n^2S_{1/2}) + Y^+ \rightarrow X^+ + Y(n^2P_{1/2,3/2})$.

b) State-to-state resolved collision cross-sections

Thanks to the high resolution provided by the 50 cm path monochromator, the different J-states from the decay signal, for the Na($3^2P_{1/2,3/2}$)[13], Rb($5^2P_{1/2,3/2}$)[14] and Cs($7^2P_{1/2,3/2}$)[15] cases (in $X + X^+$ and $X + Y^+$ collisions), could be resolved. The corresponding branching ratios (R), along with their dependence on collision energy, were derived from these measurements.

The branching ratio for the Na($3^2P_{3/2}$)/Na($3^2P_{1/2}$) case (which includes both the electron excitation and the electron capture processes) leads to values close to statistical predictions ($R=2$), especially at high collision energies. Conversely, at low energies the $J=1/2$ state becomes more readily populated. Some undulations are observed in this regime, over an essentially constant energy dependence, even though they are smaller than the experimental error bars.

A population inversion is observed in the Rb($5^2P_{3/2,1/2}$) decay signals (coming also from either direct excitation or electron capture) at about $200 \cdot 10^{-9} \text{ sm}^{-1}$ (the energy dependence is usually at its clearest when the cross-section is plotted as a function of inverse velocity), whereas R values become lower at the remaining inverse velocities. Undulations are also present, even more pronounced than in the previous case, though still too faint to draw conclusions.

The Cs($7^2P_{3/2}$)/Cs($7^2P_{1/2}$) case shows, instead, a strong dependence on inverse velocity. However, the most notable result, as for undulations in the state-to-state cross-section, is for the Rb + Cs $^+$ collision, where energy dependence enabled fitting to an analytical expression, a product of an exponentially decaying function times a sinusoidal term. This result is shown in Figure 3.

c) Magnetic (M_J -state) resolved collision cross-sections

As stated above, the experimental set-up is composed of high-resolution, high-sensitivity devices. Actual sensitivity is sufficient, in principle, to allow for the measurement of cross-sections for transitions between the different magnetic M_J sublevels. This measurement requires placing a polarising filter along the emission beam path. However, the optical system generates, during its operation, a spurious polarization signal, which has to be subtracted from the true signal arising from the collision process. An accurate measurement of the spurious polarization may be obtained from a transition whose intensity is, because of strong physical and theoretical reasons, non-polarized [16]. This non-polarized transition takes place at similar wavelengths to those under study, so that the system's operation can be checked under as similar conditions as possible. The polarization intensity obtained in this case is then assumed to correspond fully to the spurious signal, whose value is to be subtracted from the polarization intensities measured in each relevant case [14, 17–19]. This procedure is, in short, that used in the present measurements of polarization cross-sections.

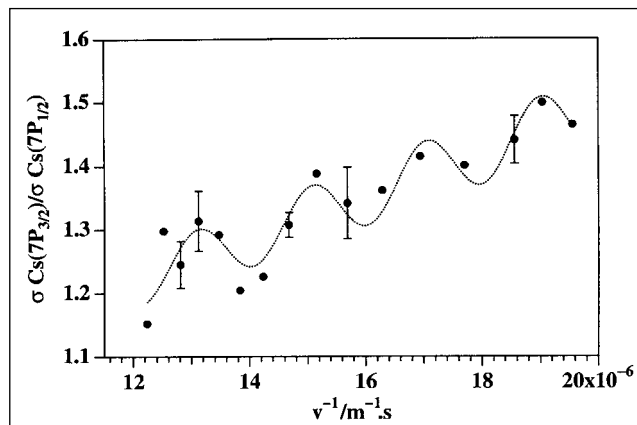


Figure 3. Branching ratio for electron capture cross-sections between Cs($7^2P_{1/2}$) and Cs($7^2P_{3/2}$), for Rb($5^2S_{1/2}$) + Cs $^+$ collisions, as a function of inverse velocity. The dotted curve represents the best fit to experimental data (solid circles), as obtained from an equation proposed in V. Aquilanti and P. Casavecchia, J. Chem. Phys. **64** (1976) 751.

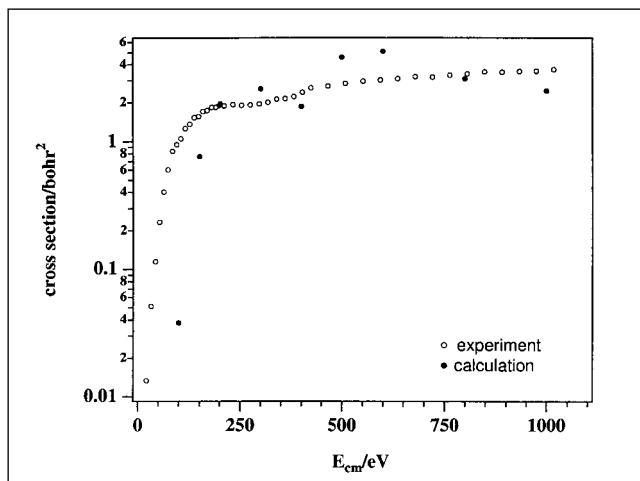
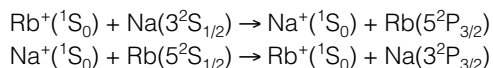
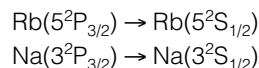


Figure 4. Hemiquantum calculations (solid circles) and experimental cross-sections (open circles), as a function of collision energy, for the electronic excitation process $\text{Rb}^+(^1\text{S}_0) + \text{Na}(3^2\text{S}_{1/2}) \rightarrow \text{Rb}^+(^1\text{S}_0) + \text{Na}(3^2\text{P}_{3/2, 1/2})$.

Collision processes for which the original signal was intense enough to allow for polarization intensity measurements are the following:



although the luminescent polarized emitting transitions for the two collision systems, respectively, are:



The spurious polarization signal is measured from the signals corresponding to the $\text{Rb}(5^2\text{P}_{1/2}) \rightarrow \text{Rb}(5^2\text{S}_{1/2})$ and the $\text{Na}(3^2\text{P}_{1/2}) \rightarrow \text{Na}(3^2\text{S}_{1/2})$ spectral line real polarization intensities, since theoretical arguments show that their polarization should be exactly zero. After an adequate deconvolution process, the whole set of M_J -selected collision cross-sections for the above systems is provided. It is worth noting that this kind of measurement is rare in the literature (even rarer in collision processes), which vouches for the usefulness of running these experiments.

d) Hemiquantum calculations and discussion

Hemiquantum methodology is reliable in the reproduction of the basic experimental features [20]. For instance, Figure 4 compares measured *versus* calculated cross-sections for the $\text{Rb}^+(^1\text{S}_0) + \text{Na}(3^2\text{S}_{1/2}) \rightarrow \text{Rb}^+(^1\text{S}_0) + \text{Na}(3^2\text{P}_{1/2})$ process. Good agreement is found, especially as only radial couplings were explicitly considered in the dynamics calculations.

Somewhat more elaborate studies were performed for processes involving the $(\text{CsNa})^+$ quasimolecule. The adia-

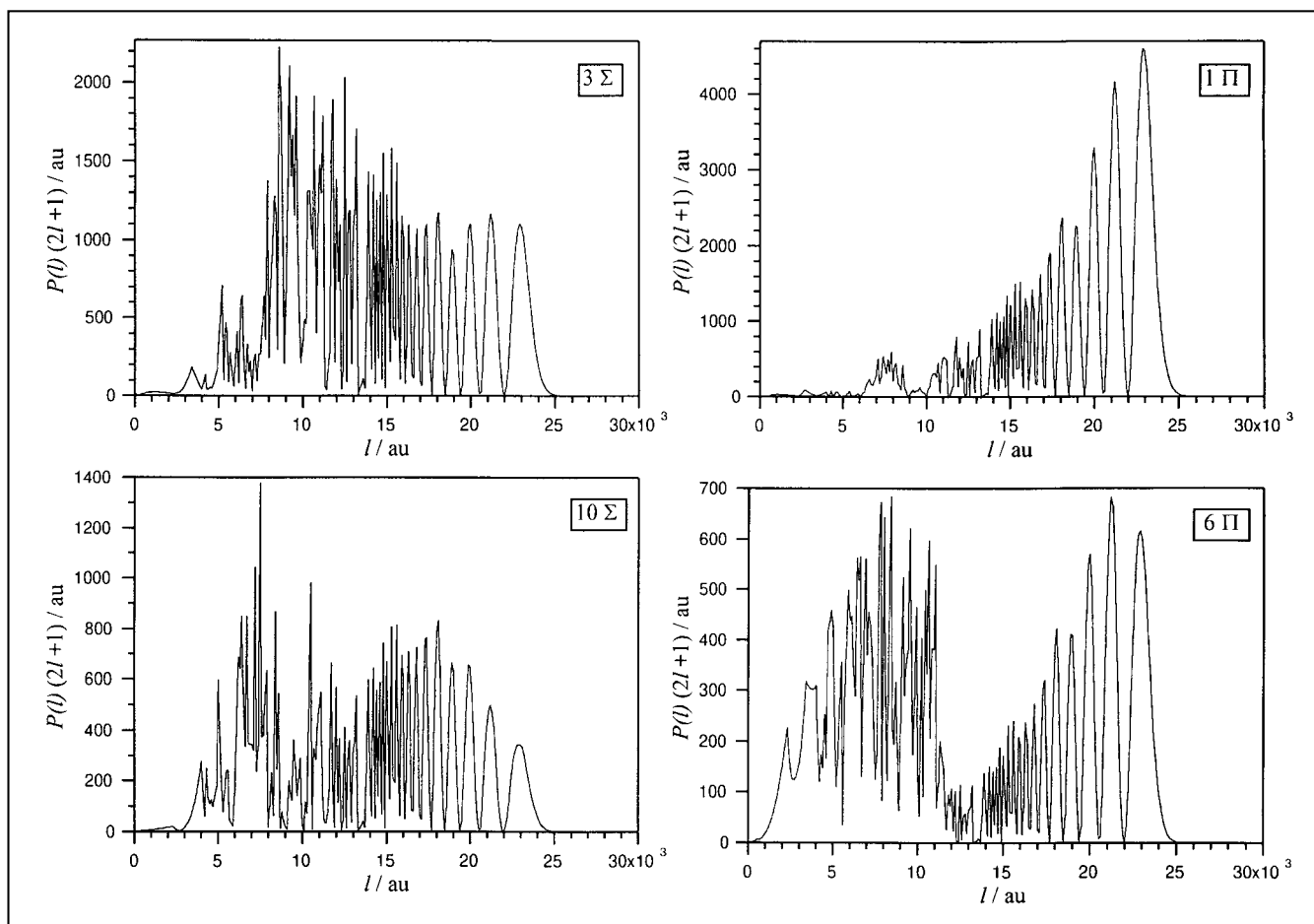


Figure 5. Hemiquantum calculations of opacity functions for the $(\text{CsNa})^+$ colliding system, for several final electronic states. Note the strongly structured behavior as a function of the orbital angular momentum.

Table 2. Hemiquantum cross-section values for the formation of different atomic states of Cs and Na in collisions between Cs and Na+ in their respective ground electronic states. Cross-sections are given in 10^{-15} cm^2 .

ECMF/eV	$\sigma(\text{Na}(3s^2S))$	$\sigma(\text{Cs}(6s^2S))$	$\sigma(\text{Cs}(6p^2P))$	$\sigma(\text{Cs}(7p^2P))$	$\sigma(\text{Na}(3p^2P))$	$\sigma(\text{Na}(4d^2D))$	$\sigma(\text{Na}(3d^2D))$
425	3.0	29.0	1.25	0.91	2.40	0.807	4.09
600	2.0	31.0	1.77	1.22	3.04	1.28	6.76
770	1.7	36.0	1.95	1.38	3.16	2.32	7.74
850	1.6	43.0	2.07	1.47	3.29	2.73	8.06
1025	1.3	46.0	2.45	1.46	3.24	3.47	8.33
1195	1.2	43.0	2.68	1.51	3.19	4.06	8.11
1275	1.2	45.0	2.89	1.65	3.30	4.50	8.09

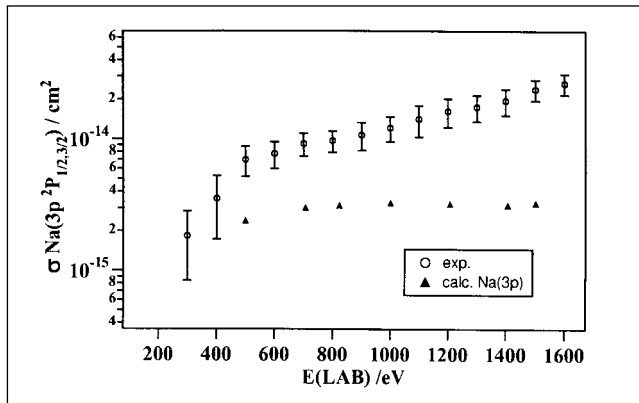


Figure 6. Experimental and calculated emission (Na 3p) cross-sections for Na ($3p^2P_{1/2,3/2}$) in the Cs ($6^2S_{1/2}$)+Na+ collision system, as a function of collision energy.

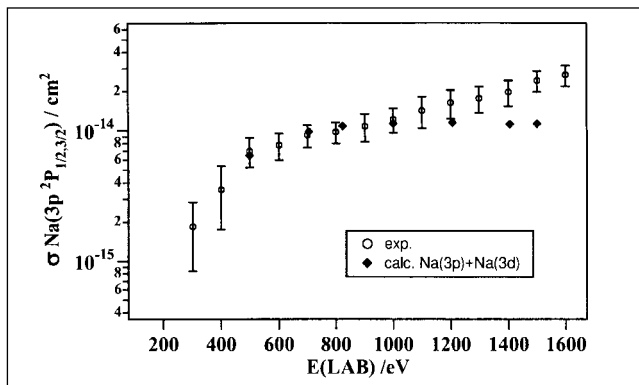


Figure 7. Experimental and calculated emission (Na 3p + Na 3d) cross-sections for Na ($3p^2P_{1/2,3/2}$) in the Cs ($6^2S_{1/2}$)+Na+ collision system, as a function of collision energy.

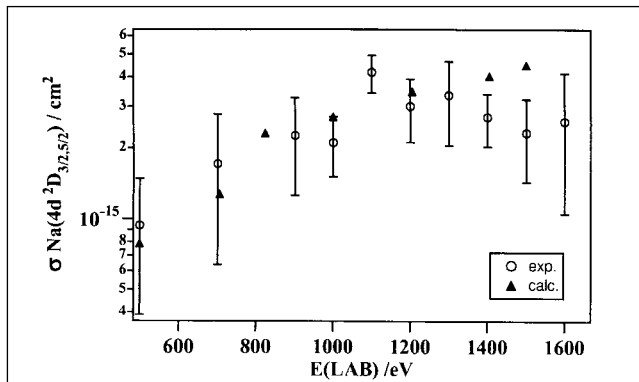


Figure 8. Experimental and calculated emission cross-sections for Na ($4p^2D_{3/2,5/2}$) in the Cs ($6^2S_{1/2}$)+Na+ collision system, as a function of collision energy.

batic expansion included 18 $^2\Sigma^+$ states and 12 $^2\Pi$, whereas the dynamical calculations were done at eight collision energies, in the low experimental energy range. Opacity functions for the Cs($6s^1,^2\Sigma^+$) + Na+($3s^0,^1\Sigma^+$) \rightarrow Cs($7p^1,10^2\Sigma^+$ and $6^2\Pi$) + Na+($3p^1,3^2\Sigma^+$ and $1^2\Pi$) are shown in Figure 5. In this process, symbols between parentheses indicate first the electronic configuration and, second, the quasimolecular state into which that configuration correlates. A first remarkable feature is the strong oscillatory behavior of the opacity function, clearly expectable from the quantum mechanical features of the electronic subsystem. Total cross-sections, for all collision channels and a given energy, are shown in Table 2. Results include processes observed experimentally, as well as unobserved channels such as Na($3d^1,^2D$). Comparisons between theory and experiment are difficult for this system. For instance, calculated cross-sections for the process leading to Cs($6p^1,^2P_{1/2,3/2}$) cannot be fully compared with experiments, since only the $J=3/2$ component could be measured. This partially explains why the calculated cross-sections are about one order of magnitude larger than the experimental values.

Charge transfer processes for the (CsNa)+ system were also analyzed. Calculated *versus* experimental cross-sections for the process leading to Na($3s^1,^2P_{1/2,3/2}$) are shown in Figure 6. An important inconsistency for the whole energy range was found. This may be explained by the contribution of cascade effects to the experimental values, since the theoretical calculations do not include this effect. This hypothesis is supported by a correction for the cascade effect from the ($4d^1,^2D_{3/2,5/2}$) state. Much greater consistency between measured and calculated cross-sections is then obtained, as shown in Figure 7, as well as for charge transfer processes leading to Na($4d^1,^2D_{3/2,5/2}$), as shown in Figure 8.

Obviously, theoretical calculations make more detailed analysis possible. For instance, the contributions from the radial ($\Sigma^+ - \Sigma^+$) and the angular ($\Sigma^+ - \Pi$) non-adiabatic couplings may be singled out. Particularly interesting is the angular part, frequently ignored in this kind of calculation, which contributes 47% to the cross-section leading to Cs($7p^1,^2P$), but as much as 87% in the process leading to Cs($6p^1,^2P$). Total elastic cross-sections, as well as charge transfer processes leading to dark channels, can also be analyzed. Elastic cross-sections are found to be one order of magnitude larger than any inelastic processes, showing the well-known dominance of elastic collisions, whereas the

dark channel is shown to contribute to the cross-section like the former luminescent transitions (see Table 2).

B. Theoretical studies of three-, four- and five-center chemical reactions

The section title stresses the kinds of systems (atom groupings) in which several techniques were applied, with the aims stated in the introduction. Results will be described according to the methodologies.

i) Development of new methods

Some of the calculations shown here tested new methods developed by the authors (or by other research groups in close collaboration).

The first case concerns the applications of NIPs to a propagation-based scattering method. Its main advantage is that the inclusion of a NIP greatly reduces the configuration space to be scanned by the propagation. This is so, since the basic idea of the method is to absorb the reactive flux (a task which is performed by the NIP) right after the transition state (TS), just when the collision starts probing the products region. This idea was introduced by Neuhauser and Baer in 1989 [8], our main contribution being its casting into a time-independent, propagation-based method [21, 22]. The price to be paid for the reduction in computational effort is that no state-to-state information is available. One has then to focus on state-selected (but not state-specific) quantities.

The incorporation of the NIP required modifying the basic formulas for the propagation methods, since a complex interaction matrix (instead of a real one) had to be propagated. It also required eliminating the coordinate transformation between reactants and products, actually a simplification. The whole transformation resulted in a computational code which performed much better than previous techniques, while accuracy was rigorously maintained. Table 3 shows CPU times for the application of the new method to the Cl + HCl symmetric exchange reaction [21]. Tests on other more general systems show that average reduction factors of four

Table 3. Convergence table for the Cl + HCl system ($E = 0.6$ eV). Relative errors are given, taking the results for $NTS = 300$ and $NV = 30$ as the exact value. Figures in bold are for results obtained with the traditional method. NTS refers to the number of sectors into which the radial coordinate is divided during the propagation stage. NV stands for the number of vibrational base functions used within each propagation sector.

<i>NTS</i>	<i>NV</i>	<i>Error %</i>	<i>CPU Time / s</i>
300	30	...	3508
300	15	0.00	756
300	10	0.00	389
300	7	0.03	258
200	15	0.13	503
200	10	0.13	261
200	7	31.00	152
150	15	0.30	378
150	10	0.30	194
150	7	32.00	113
400	27	...	1174

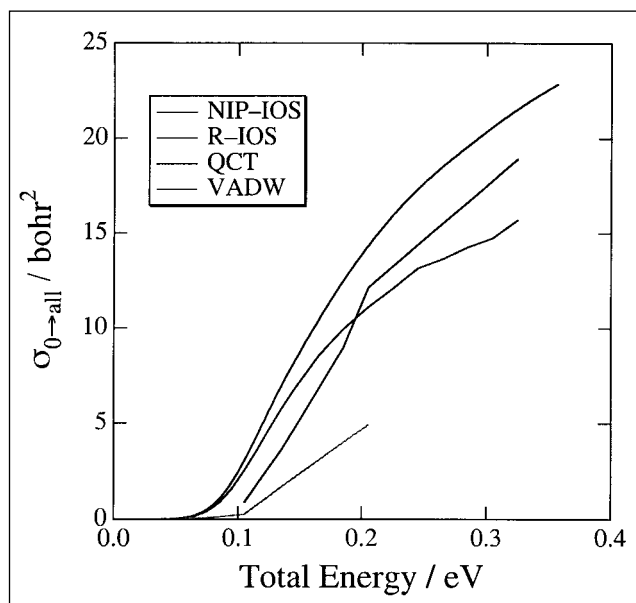


Figure 9. Integral cross-sections as a function of total energy, for the $H + F_2 \rightarrow HF + H$ reaction. NIP-IOS stands for the new, NIP-based propagation method, which is an extension of the R-IOS method. QCT corresponds to quasi-classical trajectory results, while VADW stands for Vibrationally Adiabatic Distorted Wave, a quantum perturbative method which is a more approximate quantum perturbative method.

for CPU time and of five for core memory have been obtained so far. Figure 9 shows the application of the method to the $H + F_2$ reaction, an especially favorable case since, as it is exothermic, the saved channel (products) is what actually bears the major computational overload to the calculation [23].

The second case concerns the formulation of an Infinite Order Sudden (IOS)-type method, intended for the study of pentaatomic systems, based on three main issues (previously used in simpler versions, applicable to three- and four-atom processes): a) the division of the collision problem in a reference plus a correction contribution, b) the application of a variational, Kohn-type method to get the scattering equations, and c) the use of NIPs in selected portions of configuration space, to reduce the base dimension associated with several dofs.

The purpose of this development was to allow treatment of more complex systems. In particular, as stated, the code made treatment of five-atom systems possible. The formulation was based on a reduction dimensionality scheme, by which the distances in the Hamiltonian were maintained (and thus treated in a full dynamical sense), whereas the angles were considered to be frozen during the collision (except one azimuthal angle, which was averaged when the PES was computed). A further average was then worked out on the basis of collisions at several angles (whose respective ranges are scanned in order to establish the proper interval contributing to reactivity).

The result makes available a computational code, applied by the authors to the four-dimensional study of the $C_2H + H_2 \rightarrow H_2C_2 + H$ reaction [24], the benchmark of pentaatomic

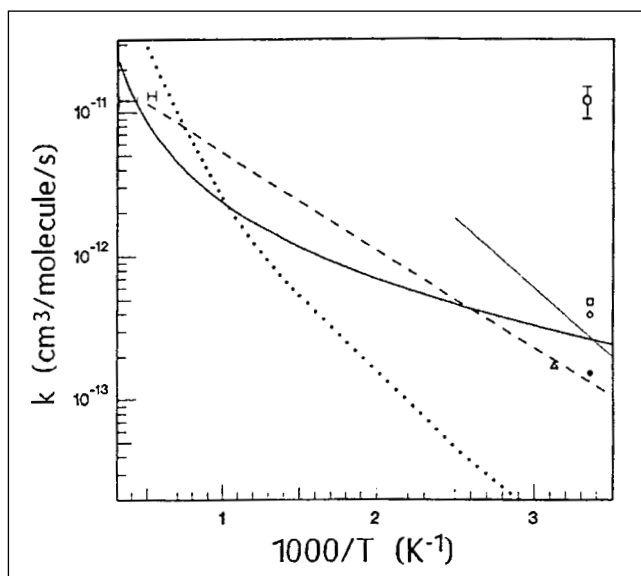


Figure 10. Arrhenius plot of the rate constant k versus $1000/T$ for the $C_2H + H_2 \rightarrow C_2H_2 + H$ reaction. The full line indicates results obtained by the authors using the pentaatomic IOS-type method. The remaining traces correspond to less accurate previous results, whereas markers correspond to different experimental measurements.

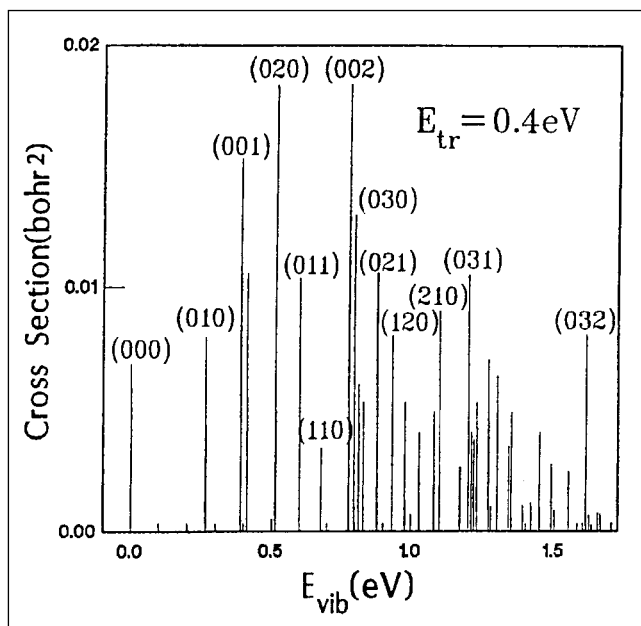


Figure 11. Vibrational state-to-state cross-sections, as a function of product vibrational energy, obtained from the state-to-state improvement of the five-atom IOS-type method. Numbers in parentheses indicate the product molecule vibrational quantum number set (simplified to symmetric stretching, one bending and asymmetric stretching, respectively).

systems. This has been the most complex study performed on a pentaatomic system to date. Results focus on the role played by the spectator bonds, i.e. those not participating in the bond breaking / formation which identifies the specific chemical reaction taking place. Figure 10 shows the result of the first study, focusing on general integral cross-sections (i.e. summed over product states) and rate constants. The second study focused on state-to-state quantities. This re-

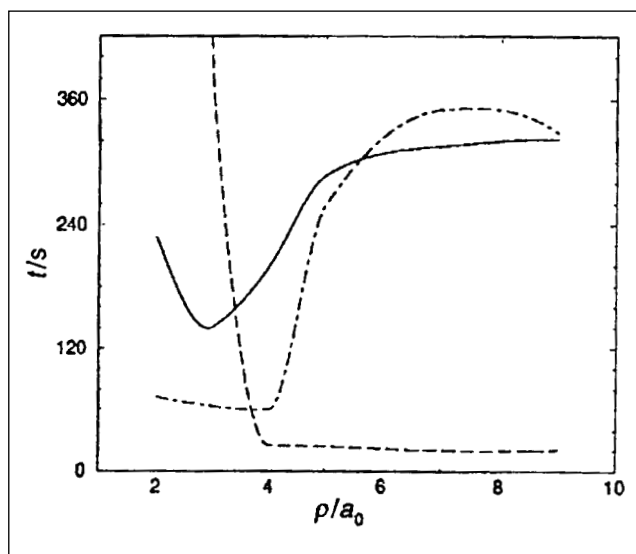


Figure 12. CPU time comparison of the Diagonalization-Truncation (DT) procedure between the two Hamiltonian representations which result from applying the DT scheme first to one or other of the internal hyperangular variables (dashed lines). Times refer to the calculation of 150 rovibrational adiabatic eigenstates and their eigenvectors. The trend without DT is also shown as an unbroken line. The conclusion is that the best strategy consists of switching from one DT scheme to the alternative, right before $4a_0$.

quired an important modification of the code, since product vibrational states had to be characterized prior to any dynamical calculation [25]. Figure 11 shows some of the state-specific integral cross-section thus obtained. Especially remarkable is the pronounced specificity of the reaction, although it is smaller than that predicted by a less accurate previous study [26].

A third development concerns our participation in implementing the Hyperquantization Algorithm (HA) [10, 27, 28] in a propagation-based scattering program. As this is an exact method for triatomic systems, as presently formulated, our main goal was easy applicability and numerical (computational) performance. Central to this was the introduction of a sequential diagonalization-truncation (DT) scheme to render the whole HA method more competitive than previous implementations of the Hyperspherical approach [29]. Figure 12 shows the reduction in computer time resulting from the DT scheme. Specific results, obtained for the $F + H_2$ system, will be discussed in the next section, since they are important in themselves (benchmark results and a rigorous comparison with experimental information), and not merely as an illustration of a given method's performance.

ii) The benchmark $F + H_2$ system

An important part of the results obtained from the application of the HA-propagative Hyperspherical method concerns the $F + H_2 \rightarrow FH + H$ reaction [28-30]. This process has been the focus of intense effort over the last 20 years, both theoretical and computational, thanks to its feasibility for accurate computations and measurements [31]. Currently, it is considered a reference system, a paradigm of the comparison between experiment and theory.

As stated, calculations on this system are aimed at reproducing the experimental information. To this end, intense work centered on generating a very accurate *ab initio* PES. Spin-orbit effects of the reactant's F atom were also included, from an adiabatic single-surface perspective, translating into a higher barrier to reaction. Finally, long-range effects, describing an entrance valley van der Waals complex, were incorporated to the surface directly from inelastic scattering measurements. The resulting general PES was used to generate general integral cross-sections at a large set of collision energies, as well as state-specific and general differential cross-sections at selected translational energies.

Figure 13 shows the general integral cross-section plotted as a function of collision energy and compared to absolute measurements from molecular beam experiments [30]. Results show that, even if consistency is quite satisfactory, some discrepancies still persist, making the theoretical curve stand shifted in energy, more towards higher values than the experimental one. This indicates that the reaction barrier has the adequate topology, but is still slightly over-estimated.

Given the enormous effort over a long period, the present discrepancies for this reaction show clearly the huge com-

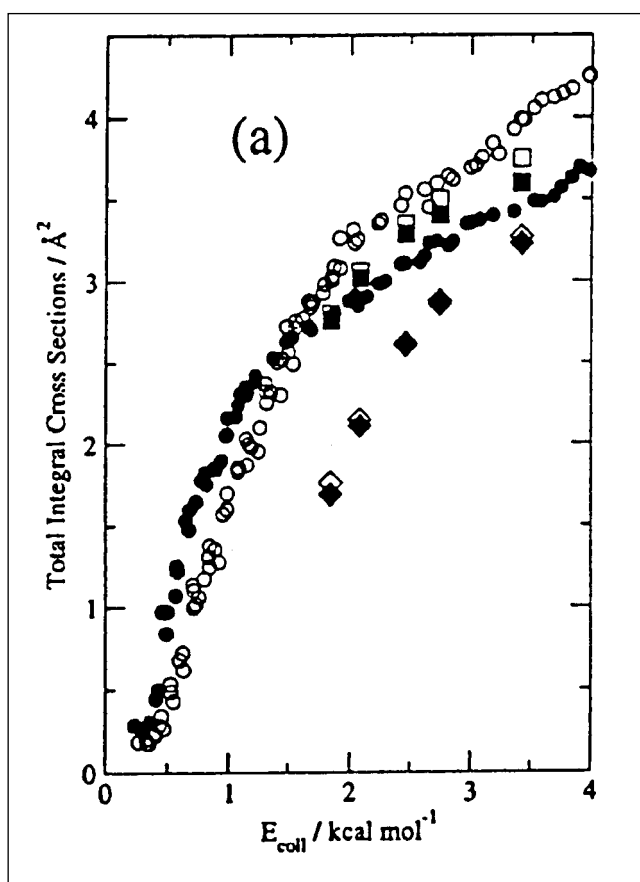


Figure 13. Total integral cross-section, as a function of collision energy, for the $F + H_2 \rightarrow FH + H$ reaction. Theoretical calculations, corresponding to two different PESs, are shown by squares (*ab initio*) and by diamonds (more accurate *ab initio* + spin orbit + long range). Experimental results correspond to circles. The discrepancy between the most accurate PES (diamonds) and experiments tells that further work on the PES is necessary, in particular concerning the barrier height.

lications that the quantitative prediction of chemical reactivity involves. Actually, it is impressive that *absolute measurements* compare so well to *ab initio structure + dynamics calculations* (i.e. no parametrizations, no relative measurements, etc.). However, the extremely small energies controlling the reactive event, along with the large amplitude motions involved in the corresponding rearrangement, prevent full consistency between theory and experiment. But it is not only theoretical calculations that need to be improved. If the cross-sections available in the literature are compared as a function of energy, as well as the available rate constants, it is found that the two sets of data, which come from different experimental set-ups, are actually inconsistent, since cross-sections are higher than theoretical predictions, whereas rate constants are lower than the calculations themselves. Clarification is essential.

Fuller *ab initio* calculations on the PES are currently underway, focusing mainly on barrier height [32]. Once these are available, new dynamics calculations will be carried out. Concurrently, the possible influence of excited energy surfaces is being assessed from a non-adiabatic perspective. The (relatively) small current discrepancies and the work under way at present lead us to think that the full dynamics problem may be essentially solved in the near future. If so, a milestone in the history of our field will be reached.

iii) Accurate study of quantum effects: the $Ne + H_2^+$, $He + H_2^+$ and $BO + H_2$ systems

The accurate characterization of quantum effects in reactive collisions is one of the hot topics in the field. They are mainly (but not exclusively!) identified as tunneling, zero point energy (ZPE) and reactive scattering resonances (RSR) [33]. Tunneling is usually singled out as a non-Arrhenius curvature in the rate constant plot *versus* temperature. However, it is actually a much more complex process, whose full nature is not completely understood. However, the effect of ZPE is a shift towards higher values of the reactivity threshold as a function of energy, i.e. the dynamical trapping of a given amount of energy as ZPE is subtracted from the energy available to reaction. Finally, RSRs look like being the most elusive of the quantum features. They correspond to quasi-trapped, metastable scattering states, which lead to strong oscillations (actually, spikes, shoulders, troughs, ...) in the reaction probability profile as a function of energy. Since the cross-sections are obtained from probability as a sum of all values contributing to the total angular momentum, it is frequently argued that this sum might quench any existing structure in the probability profile. However, as it becomes possible to treat more complex systems by quantum scattering methods, it has been found that in given cases RSRs are so intense and sharp (i.e. strongly bound) that they do survive angular momentum averaging. The conclusion is that this quantum effect is much more relevant than expected, thus deserving much greater attention, since it may strongly influence the absolute value of cross-sections and rate constants.

The desire to account fully for quantum effects triggered the study of the $Ne + H_2^+ \rightarrow NeH^+ + H$ endothermic, ion-mol-

ecule reaction. This system is characterized by the presence of a stable intermediate complex, which strongly mediates in the quasi-trapped states formation. Previous experience of this system had shown that the reaction probability profile was plagued with intense resonant peaks, as a function of energy, for zero total angular momentum. At this point, the authors performed a numerically converged full-dimensional cross-section calculation, scanning a fine energy mesh to search for the possible survival of resonant structures at the cross-section level [34, 35]. Figure 14 gives the results of this calculation and shows that, in the low-energy regime, RSRs are far from being quenched. Actually, a peak as high as 5 \AA^2 (over the background reactivity) is obtained. The main conclusion is that this feature seems to be detectable by means of current, highly energy-selective molecular-beam methods.

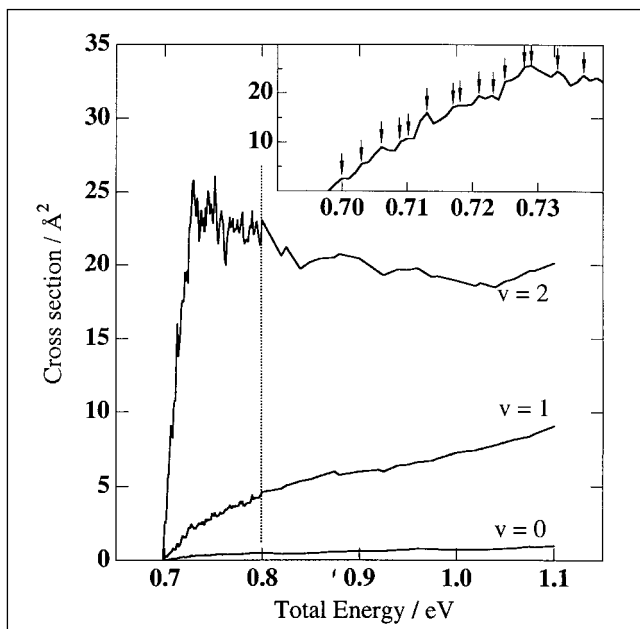


Figure 14. State-to-all integral cross-section, as a function of total energy, for the first three ($v,j=0$) rovibrational levels, for the $\text{Ne} + \text{H}_2^+ \rightarrow \text{NeH}^+ + \text{H}$ reaction. The inset shows an enlargement of the threshold region for the $v=2$ case, where the arrows show the progression in the cross-section maxima. The vertical dashed line at 0.8 eV separates the fine and coarse regions in the energy scanning: 100 equally spaced energy values were included up to 0.8 eV, whereas 25 energies were from 0.8 to 1.1 eV.

The experimental search for RSRs is, however, a truly gigantic task, as is its eventual reproduction at the theoretical level. The reason is that RSRs are extremely sensitive to the PES shape. To prove this, the authors engaged on a detailed study of a reaction belonging to the same family, $\text{He} + \text{H}_2^+ \rightarrow \text{HeH}^+ + \text{H}$, since this reaction has the added advantage of very high accuracy, as the PES involves calculations with only three electrons. A preliminary study demonstrated the high sensitivity of the PES, even in the specific fitting procedure used to get a function from the *ab initio* mesh [36]. It was found that, on slightly changing either the surface or the fitting, the resonance pattern changed completely. This result prompted a further study, by which a new *ab initio* mesh

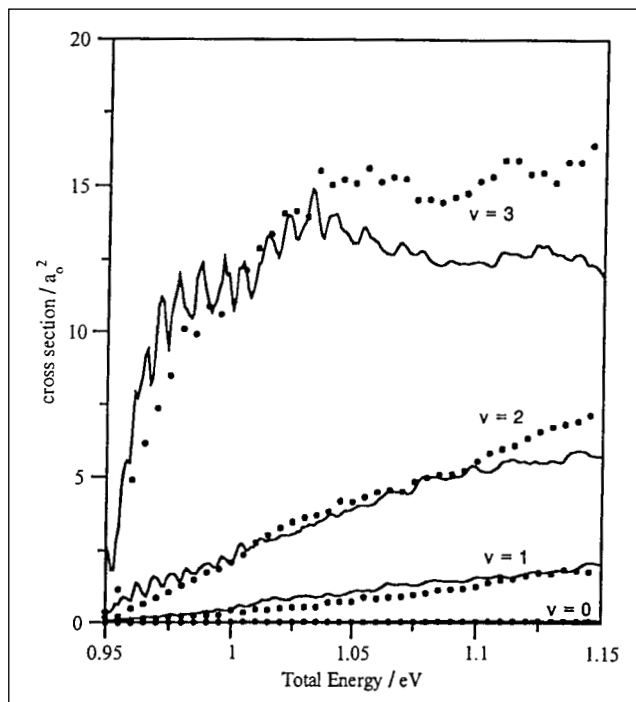


Figure 15. Integral cross-section as a function of total energy for the reaction $\text{He} + \text{H}_2^+ \rightarrow \text{HeH}^+ + \text{H}$, summed over all open final rotational states, on a new PES generated from an accurate mesh of *ab initio* points.

was generated, using a more refined quantum chemistry method. The new mesh, along with a more accurate fit, let a new set of cross-sections be created at several energy values (see Figure 15) [37]. These results look more stable against a change in the PES fitting procedure, so should be more robust in future comparisons with accurate experimental information.

The description of our search for characterizing quantum effects is completed here by a multidimensional study of tunneling, performed on the $\text{BO} + \text{H}_2 \rightarrow \text{HBO} + \text{H}$ reaction. As a scattering code for reduced dimensionality studies for tetraatomic systems was available, we used it to explore the

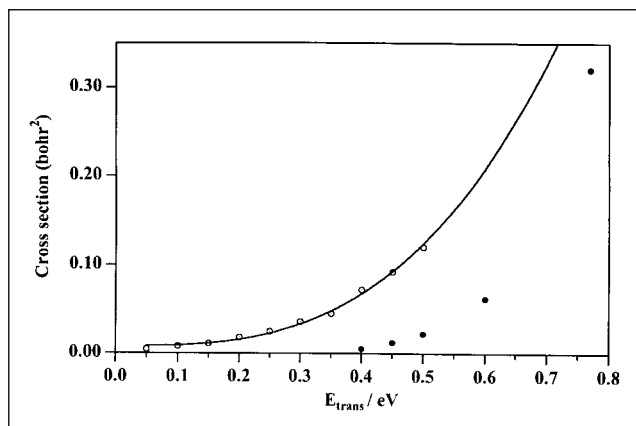


Figure 16. A comparison between integral cross-sections corresponding to a four-atom IOS-type quantum mechanical method (open circles) and the QCT method (full circles). Cross-sections below 0.4 eV correspond to purely under-barrier tunneling contributions. The continuous line is shown only to help viewing.

above reaction: previous evidence, based on transition state theory estimates, plus tunneling corrections, showed that the latter might be rather significant. Thus, we performed a 3D-accurate, 6D-approximate calculation of the reactive cross-section as a function of energy [38]. The results of this clearly show that the tunneling contribution to reactivity is actually much larger than previously expected (Figure 16). The result is even more remarkable in view of the scarcity of moderately accurate estimations of high-dimensional tunneling processes, and the estimations that, the higher the dimensionality of the problem, the smaller it should be. Clearly, light atom transfer, along with a sharp barrier to reaction, along the reaction coordinate, makes the tunneling contribution especially important for this process.

iv) Understanding scattering dynamics features: the $\text{Ar}^* + \text{ClF}$ and $\text{BO} + \text{H}_2$ systems

In this section, a study which is richer in its dynamical quantities examines two elementary reactions, based on studies using the quasi-classical trajectory method.

The first process concerns the excited state, two-product channel, exothermic $\text{Ar}^* + \text{ClF} \rightarrow \text{ArCl}^* + \text{F}$, $\text{ArF}^* + \text{Cl}$ rare-gas halide reaction. Cross-sections, rate constants and products' energy disposal for both ArCl^* and ArF^* excimer formation were calculated [39] (the asterisk indicates the Ar atom in an initially excited electronic state, and the formation of the molecular species in an excited rovibrational state), showing a dominance of the less stable $\text{ArCl}^* + \text{F}$ channel. Specifically, integral cross-sections as a function of energy are shown in Figure 17, showing that the total cross-section arises as the sum of a decreasing (with energy) contribution from the ArCl^* , plus an increasing contribution from the ArF^* channel. Both trends are easily explained in terms of the PES topography. A remarkable enhancing effect of reactant rotation, as compared to vibration, was found for the ArCl^* product, whereas the opposite trend was observed for the ArF^* channel. This behavior can be explained in terms of kinematic (mass-related) considerations. The effect of rotational excitation was also used to clarify the angular momentum

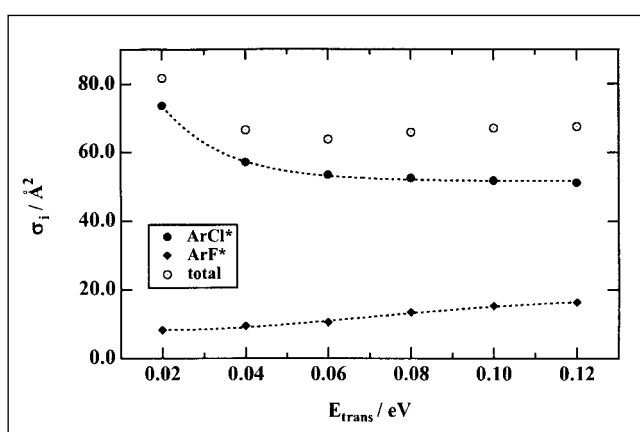


Figure 17. Total and partial (as for product arrangements) reaction cross-sections, σ_i ($i = \text{ArCl}^*$, ArF^*) as a function of reactant translational energy, for the ($v = 0$, $J = 14$) reactant rovibrational state. Lines are shown only to help viewing.

transfer mechanism between the two competing reaction channels. A non-negligible orbital-rotational angular momentum coupling, from which a simple rotor dynamics model was worked out to interpret the impact parameter dependence on reactant rotation, was identified. In general, results seem to indicate that a single-value surface, constructed with the inclusion of the main characteristics of the reaction mode observed for similar reactions, describes the dynamics of the ArCl^* and ArF^* excimer formation in the $\text{Ar}(^3\text{P}) + \text{ClF}$ colliding system.

The second study is devoted to the function of the spectator bond in the tetra-atomic $\text{BO} + \text{H}_2 \rightarrow \text{HBO} + \text{H}$ reaction. Previous evidence from similar reactions pointed to a prospective proportionality between the amount of inhibition, when the non-reactive bond was vibrationally excited, and the mass of one of the spectator atoms [40]. The specific purpose of this research was then to shed light on this proportionality. To this end, the B and O masses were artificially doubled and halved, so as to check the resulting isotopic effect [41]. Contrary to prior expectations, the presumed proportionality clearly failed. Actually, an interesting effect was observed instead. It was found that a *decrease* in the reduced BO mass *diminished* reactivity (i.e. the cross-section) when the BO molecule was initially in excited vibrational states. However, the *very same decrease* in the BO reduced mass was found to *promote* reactivity when the molecule initially excited (with vibration) was H_2 . This apparent counter-intuitive behavior was satisfactorily explained by assuming the intervention, in the reaction mechanism, of TS normal modes other than those correlating with the initial reactant modes. In particular, data are explained by assuming that rotation-related modes actively participate in the reaction. This leads to a complete breakdown of the spectator bond mechanism, often used for explaining reactivity trends in several polyatomic reactions.

V. Future prospects

Our research group is involved in new projects which seek to extend earlier studies to more complex collision and chemical systems.

On the experimental side, future studies include the use of alkali-earth atom targets, for which some preliminary results actually exist, as for the ion-atom collision line. Concurrently, a new apparatus has recently been assembled to study ion-molecule collisions, thus opening up the possibility of studying molecular dissociation and ionization. Stable target beams of ZnCl_2 , SnCl_2 and CdI_2 have already been successfully generated, and even excited Na and Cl^+ bands from $\text{SnCl}_2 + \text{Na}^+$ collisions have been found. Reaction products might be analyzed once a mass analysis system, currently being assembled, is available.

The experimental study of reactive ion-molecule collisions requires, however, very low ion energies. This fact prevents both the generation and focusing of the corresponding beams, under the current experimental set-up. For this rea-

son, a modified apparatus is now under construction. It is based on directing a low-energy ion beam towards an octupolar electromagnetic field, which is able to guide and focus it. The octupolar field generator is enclosed in a sleeve, into which a suitable gas is injected. Ions ejected from the octupole will be mass-analyzed, and the decay fluorescence collected and analyzed. The operation of the octupole has already been successfully tested.

Finally, a third machine, for the experimental study of collisions involving excited atoms, is under construction. This apparatus will generate beams of metastable excited rare gas atoms, using a standard set-up mounted in a differentially pumped chamber. This will be fed into another chamber and crossed with suitable targets. Again, both fluorescence and mass analysis will be used to characterize the collision processes.

On the theoretical side, the recent availability of computer codes based on a different theoretical framework, the semi-classical approach, is expected to make it possible to perform scattering studies on more complex polyatomic systems and eventually examine the corresponding reactions in the condensed phase. These studies look possible thanks to the smaller computational needs of the semi-classical approach, since they are based on the computation of classical trajectories. But, at the same time, quantum effects are taken into account, at least semi-quantitatively, thanks to the fact that quantum algebra, under the stationary phase approximation, is used to compute any required quantity. This means, ultimately, that quantum mechanical amplitudes are computed by accumulating a sum of classical actions and stability matrices, thus obtaining interference, the origin of any quantum effect. Work on some fundamental aspects of the method has already been performed [42-44], and we expect to report soon on progress in specific applications.

At the same time, the rigorous quantum mechanical studies of benchmark systems are to be continued. Currently, further refinements of the $F + H_2$ PES suggest greater accuracy can be reached, while new calculations on the $O^+ + H_2$ system, on a new PES, are currently underway. Preliminary results are very encouraging.

VI. Summary and conclusions

The experimental and theoretical work of the authors during the last five years are extensively reviewed in this paper.

The experimental part focuses on intermediate energy ion-atom collision processes, for which both direct excitation and charge transfer processes were measured for virtually all combinations of alkali ions and alkali atoms. These studies complete a series started some time ago. In addition, carefully selected and highly sensitive new measurements, discerning the spin-orbit components and even the magnetic sublevels, were provided for the first time. Results were interpreted in terms of simple non-adiabatic, curve-crossing models, as well as by means of more sophisticated computer simulations, using hemiquantum-type methodology. The

theoretical apparatus allowed much deeper analysis and interpretation of the experimental results, along with the characterization of several theoretical contributions (e.g. radial and angular non-adiabatic couplings) to the overall results.

The theoretical part focuses on the study of three-, four- and five-atom elementary reactive processes. The specific systems studied so far permitted: a) checking how new methods out-perform previous versions, b) verifying the accuracy of new formulations of exact methods, c) establishing the degree of accuracy of full *ab initio* studies (electronic + nuclear) for the $F + H_2$ and $He + H_2^+$ systems, d) singling out several outstanding quantum mechanical features (mainly resonances and tunneling), and e) performing extended studies on the dynamics of certain elementary chemical reactions, and interpreting the new data found in terms of simple models.

Future prospects are also given for both the experimental and the theoretical sides. In short, it is expected that more complex chemical and collision systems will be dealt with in the near future.

Acknowledgements

The authors are grateful to the many researchers with whom it has been a pleasure to work through the years. Among these, special thanks are given to their former Ph.D. students M.E. Aricha, J.M. Bocanegra, R. Blasco, F. Huarte-Larrañaga, M. Prieto, T. Romero, A. Salich and J. Sogas, to the senior researchers M. Gilibert and A. Volpi, and to Professors M. González, R. Sayós, J.M. Alvaríño, V. Aquilanti, M. Baer, B. Brunetti, S. Cavalli, D. de Fazio, F.X. Gadea, A. González Ureña, A. Laganà, I. Last, J.-M. Lounay, W.H. Miller, H. Szychman and F. Vecchiocattivi. Financial support from the Spanish DGICYT (projects PB94-0909, PB97-0919) and the Generalitat de Catalunya (CUR projects 1996-SGR000040, 1998-SGR00008, 2000-SGR00016) is gratefully acknowledged. Computer time was generously allocated by the Centre de Supercomputació de Catalunya (CESCA).

References

- [1] R.D. Levine and R.B. Bernstein: «Molecular reaction dynamics and chemical reactivity». Oxford U.P., Oxford, 1987.
- [2] G.D. Billing and K.V. Mikkelsen: «Advanced molecular dynamics and chemical kinetics». Wiley, New York, 1997.
- [3] J.Z.H. Zhang: «Theory and application of quantum molecular dynamics». World Scientific, Singapore, 1999.
- [4] Phys. Chem. Chem. Phys. Special issue on «Chemical reaction theory». 1 (1999).
- [5] R. Campargue (Ed.): «Atomic and molecular beams. The state of the art 2000». Springer Verlag, Berlin, 2001.

- [6] A. Aguilar, M. Albertí, J. de Andrés, M. Gilibert, X. Giménez, M. González, J.M. Lucas, M. Prieto, R. Sayós and A. Solé: «Crossed molecular beam study of the $M^+(^1S) + Na(3^2S) \rightarrow M^+(^1S) + Na(3^2P)$ collision system ($M^+ = Li^+, Na^+, K^+, Cs^+$) in the 0.05 – 3.00 keV energy range». *Chem. Phys. Lett.* 220 (1994) 267 (and references therein).
- [7] R.T. Skodje, D. Skouteris, D.E. Manolopoulos, S.-H. Lee, F. Dong and K. Liu: «Observation of a transition state resonance in the integral cross section of the $F + HD$ reaction». *J. Chem. Phys.* 112 (2000) 4536.
- [8] D. Neuhauser and M. Baer: «Wave-packet approach to treat low energy reactive systems: accurate probabilities for $H + H_2$ ». *J. Phys. Chem.* 93 (1989) 2872.
- [9] J.M. Launay and M. LeDourneuf: «Hyperspherical close coupling calculation of integral cross sections for the reaction $H + H_2 \rightarrow H_2 + H$ ». *Chem. Phys. Lett.* 163 (1989) 178.
- [10] V. Aquilanti, S. Cavalli and M. Monnerville: «The hyperquantization algorithm: the use of discrete analogs of hyperspherical harmonics for reactive scattering». In C. Cerjan (Ed.): «Numerical grid methods and their application to Schrödinger's equation». Kluwer, The Netherlands, 1993.
- [11] L.L. Marino: «Charge transfer between alkali-metal ions and cesium atoms». *Phys. Rev.* 152 (1966) 152.
- [12] V. Aquilanti, P. Casavecchia and G. Grossi: «Cross sections for excitation of the potassium resonance doublet in collisions between potassium atoms and alkali ions». *J. Chem. Phys.* 65 (1976) 5518.
- [13] J.M. Lucas, J. de Andrés, A. Aguilar, M. Albertí, M. Prieto and T. Romero: «State-to-state crossed molecular beam measurements for collision processes in $Na / Na^+, K^+$ and Cs^+ systems». *Chem. Phys. Lett.* 238 (1995) 338.
- [14] J. de Andrés, T. Romero, A. Aguilar, M. Albertí, J.M. Lucas, J. Sogas and J.M. Bocanegra: «Electronic excitation and electron capture processes in the collision between Rb atoms and Na ions by crossed molecular beams». *Chem. Phys. Lett.* 281 (1997) 74.
- [15] M. Albertí, A. Aguilar, J.M. Lucas, J. Sogas, T. Romero, J. de Andrés, J.M. Bocanegra: «Electronic excitation and electron capture processes in $Rb(5^2S_{1/2})$ collision with Cs^+ and Li^+ ions». *Phys. Chem. Chem. Phys.* 1 (1999) 5607.
- [16] B. Brunetti, B. Elisei and C. Vergari: «A photon polarization study of the doublet emission in potassium ion-atom collisions». *Nuovo Cimento* 63 (1981) 98.
- [17] N. Bendali, N.T. Duong, P. Juncar, J. St. Jalm, J.L. Vialle: « $Na^+ - Na$ charge exchange processes studied by collinear laser spectroscopy». *J. Phys. B* 19 (1986) 233 (and references therein).
- [18] T. Romero, A. Aguilar, M. Albertí, J.M. Lucas, J. Sogas, J. de Andrés: «Electron capture processes in the collision between rubidium ions and Na neutral atoms by crossed molecular beams». *Chem. Phys. Lett.* 272 (1997) 271.
- [19] T. Romero, A. Aguilar, M. Albertí, J.M. Lucas, J. de Andrés: «Electronic excitation processes in the collisional system $Na(3^2S) + Rb^+(^1S) \rightarrow Na^+ + Rb^+(^1S)$ by crossed molecular beams in the 0.1 – 5.0 keV energy range». *Chem. Phys.* 209 (1996) 217.
- [20] M. Albertí, A. Aguilar, J.M. Lucas, J. Sogas, T. Romero, J. de Andrés, J.M. Bocanegra, F.X. Gadea: «Crossed beams and theoretical study of the $(NaRb)^+$ collisional system», in ref. [5].
- [21] F. Huarte-Larrañaga, X. Giménez, A. Aguilar and M. Baer: «On the accuracy of reactive scattering calculations with absorbing potentials: a new implementation based on a generalized R-matrix propagation». *Chem. Phys. Lett.* 291 (1998) 346.
- [22] F. Huarte-Larrañaga, X. Giménez and A. Aguilar: «The application of complex absorbing potentials to an invariant embedding scattering method: I. Theory and computational details». *J. Chem. Phys.* 109 (1998) 5761.
- [23] F. Huarte-Larrañaga, X. Giménez, J.M. Lucas and A. Aguilar: «The application of complex absorbing potentials to an invariant embedding scattering method: II. Applications». *J. Chem. Phys.* 111 (1999) 1979.
- [24] H. Szichman, M. Gilibert, M. González, X. Giménez and A. Aguilar: «Four-dimensional quantum mechanical treatment of penta-atomic systems: Case $H_2 + C_2H \rightarrow H + C_2H_2$; total reactive probabilities, cross sections and rate constants». *J. Chem. Phys.* 113 (2000) 176.
- [25] H. Szichman, M. Gilibert, M. González, X. Giménez and A. Aguilar: «A four-dimensional quantum mechanical state-to-state study of the $H_2 + C_2H \rightarrow H + C_2H_2$ reaction». *J. Chem. Phys.* 114 (2001) 9882.
- [26] D. Wang and J.M. Bowman: «Quantum calculations of unusual mode specificity in $H + C_2H_2 \rightarrow H_2 + C_2H$ ». *J. Chem. Phys.* 101 (1994) 8646.
- [27] V. Aquilanti, S. Cavalli and D. de Fazio: «Hyperquantization algorithm. I. Theory for triatomic systems». *J. Chem. Phys.* 109 (1998) 3792.
- [28] V. Aquilanti, S. Cavalli, D. de Fazio, A. Volpi, A. Aguilar, X. Giménez and J.M. Lucas: «Hyperquantization algorithm. II. Implementation for the $F + H_2$ reaction dynamics including open-shell and spin-orbit interactions». *J. Chem. Phys.* 109 (1998) 3805.
- [29] V. Aquilanti, S. Cavalli, D. de Fazio, A. Volpi, A. Aguilar, X. Giménez and J.M. Lucas: «Probabilities for the $F + H_2 \rightarrow HF + H$ reaction by the hyperquantization algorithm: alternative sequential diagonalization schemes». *Phys. Chem. Chem. Phys.* 1(1999) 1091.
- [30] V. Aquilanti, S. Cavalli, D. de Fazio, A. Volpi, A. Aguilar, X. Giménez and J.M. Lucas: «Exact reaction dynamics by the hyperquantization algorithm: integral and differential cross sections for $F + H_2$, including long-range and spin-orbit effects». *Phys. Chem. Chem. Phys.* 4 (2002) 401.
- [31] D.E. Manolopoulos: «The dynamics of the $F + H_2$ reaction». *J. Chem. Soc. Faraday Trans.* 93 (1997) 673.
- [32] D. de Fazio. Private communication.
- [33] E.J. Heller: «The many faces of tunneling». *J. Phys. Chem. A* 103 (1999) 10433.

- [34] F. Huarte-Larrañaga, X. Giménez, J.M. Lucas, A. Aguilar and J.M. Launay: «Exact quantum 3D cross sections for the $\text{Ne} + \text{H}_2^+ \rightarrow \text{NeH}^+ + \text{H}$ reaction by the hyperspherical method. Comparison with approximate quantum mechanical and classical results». *Phys. Chem. Chem. Phys.* 1 (1999) 1125.
- [35] F. Huarte-Larrañaga, X. Giménez, J.M. Lucas, A. Aguilar and J.M. Launay: «Detailed energy dependences of cross sections and rotational distributions for the $\text{Ne} + \text{H}_2^+ \rightarrow \text{NeH}^+ + \text{H}$ reaction». *J. Phys. Chem. A* 104 (2000) 10227.
- [36] V. Aquilanti, G. Capecchi, S. Cavalli, D. de Fazio, P. Palmieri, C. Puzzarini, A. Aguilar, X. Giménez, J.M. Lucas: «The $\text{He} + \text{H}_2^+$ reaction: a dynamical test on potential energy surfaces for a system exhibiting a pronounced resonance pattern». *Chem. Phys. Lett.* 318 (2000) 619.
- [37] P. Palmieri, C. Puzzarini, V. Aquilanti, G. Capecchi, S. Cavalli, D. de Fazio, A. Aguilar, X. Giménez, J.M. Lucas: «Ab initio dynamics of the $\text{He} + \text{H}_2^+ \rightarrow \text{HeH}^+ + \text{H}$ reaction: a new potential energy surface and quantum mechanical cross sections». *Mol. Phys.* 98 (2000) 1835.
- [38] H. Szychman, M. Gilibert, M. Albertí, X. Giménez and A. Aguilar: «A reduced dimensionality QM study of the $\text{BO} + \text{H}_2 \rightarrow \text{HBO} + \text{H}$ reaction: tunneling in polyatomic reactions». *Chem. Phys. Lett.* 353 (2002) 446.
- [39] J. Sogas, M. Albertí, X. Giménez and A. Aguilar: «Dynamics of excited rare-gas atoms with halide molecules: the $\text{Ar}(^3\text{P}) + \text{ClF} \rightarrow \text{ArCl}^* + \text{F}$, $\text{ArF}^* + \text{Cl}$ reaction». *J. Phys. Chem. A* 104 (2000) 10529.
- [40] J. Sogas, M. Albertí, X. Giménez, R. Sayós and A. Aguilar: «Dynamics of the four-atom $\text{BO} + \text{H}_2 \rightarrow \text{HBO} + \text{H}$ reaction: potential energy surface and reaction selectivity from QCT calculations». *J. Phys. Chem.* 101 (1997) 8877.
- [41] J. Sogas, M. Albertí, X. Giménez and A. Aguilar: «Role of the BO bond in the reactions dynamics of $\text{BO} + \text{H}_2 \rightarrow \text{HBO} + \text{H}$ ». *Chem. Phys. Lett.* 347 (2001) 451.
- [42] R. Gelabert, X. Giménez, M. Thoss, H. Wang and W.H. Miller: «A log-derivative formulation of the prefactor for the semiclassical Herman-Kluk propagator». *J. Phys. Chem. A* 104 (2000) 10321.
- [43] H. Wang, M. Thoss, K.L. Sogge, R. Gelabert, X. Giménez and W.H. Miller: «Semiclassical description of quantum coherence effects and their quenching: a forward-backward initial value representation study». *J. Chem. Phys.* 114 (2001) 2562.
- [44] R. Gelabert, X. Giménez, M. Thoss, H. Wang and W.H. Miller: «Semiclassical description of diffraction and its quenching by the forward-backward version of the initial value representation». *J. Chem. Phys.* 114 (2001) 2572.

About the authors

The members of the Kinetics and Dynamics of Elementary Reactions group involved with the research reported in this review belong to the Department of Physical Chemistry at the University of Barcelona. Their research activity focuses on both experimental and theoretical studies of the dynamics of reactive and non-reactive atomic and molecular collisions. The present review is a good source of information on the experimental methods and theoretical techniques that the authors have developed, implemented and used through the recent years.

The authors, who obtained their first degrees (except M.A., who graduated

from UNED) and their Ph. Ds. at the University of Barcelona, gained further experience during stays at Spanish and international academic and research institutions, such as the Univ. Complutense de Madrid, Univ. Autònoma de Barcelona, Univ. of Perugia (Italy), Univ. of Lisbon (Portugal), Univ. of Paris-Sud and CNRS at Meudon (France), the Academy of Sciences of Moscow (Russia) and the Univ. of California at Berkeley (USA), amounting to more than seven years in all. Research collaborations with groups from these universities are still active in several cases. Joint research is also ongoing with other outstanding researchers in the field. Some projects had their origins in visits by foreign researchers to the group's laboratory.

Current research is supported by the Generalitat de Catalunya, the Spanish Ministry of Science and Technology, the Catalan Research Foundation (Super-computation Catalan Center) and the European Union (TMR, IHP and COST programs). Every member of the group belongs to at least one of the following organizations: the Spanish Royal Societies of Physics and Chemistry, the Specialist Group of Atomic and Molecular Physics, the Chemistry Division of the Institut d'Estudis Catalans and the European Physical Society. Overall, members of the group have published more than 120 scientific papers, lectured at dozens of Universities and international meetings, and organized several international meetings and workshops.